ORIGINAL SCIENTIFIC PAPER

CROATICA CHEMICA ACTA

Croat. Chem. Acta **2025**, *98*(1), 1–14
Published online: March 27, 2025
DOI: 10.5562/cca4128

HKD 1926

3D-QSAR, Molecular Docking and ADMET Studies of Benzothiadiazinonedioxides-Triazole Derivatives Against Carbonic Anhydrase-XII

Abdelkader Naouri,[1,2,*] Oussama Abderrahmane Boudinar,[3] Mokhtar Fodili[4]

[1] Technical Platform of Physico-Chemical Analysis PTAPC-Djelfa-CRAPC, Djelfa, Algeria
[2] Centre de Recherche Scientifique et Technique en Analyses Physico-chimiques (CRAPC), BP384, Bou-Ismail, Tipaza, Algeria
[3] University of Dr Yahia Fares, Faculty of Technology, Laboratory of Materials and Environment, Urban Center, Medea, Algeria
[4] University of Djelfa, Organic Chemistry and Naturel Substances Laboratory, Djelfa, Algeria
* Corresponding author's e-mail address: aeknaouri@gmail.com, abdelkader.naouri@crapc.dz

RECEIVED: September 23, 2024 * REVISED: November 30, 2024 * ACCEPTED: December 4, 2024

Abstract: A series of novel 2H-benzo[e][1,2,4]thiadiazin-3(4H)-one-1,1-dioxides (BTDs) as *hCA* XII inhibitors with remarkable activities have been reported recently. In this study, a three-dimensional quantitative structure-activity relationship (3D-QSAR), molecular docking, ADMET and drug-likeness analyses were conducted on the reported BTDs to gain deeper insight into the key pharmacological features of *hCA* XII inhibitors and identify new potential compounds. The constructed 3D-QSAR models demonstrated reliable predictability with satisfactory validation parameters. Including $Q^2 = 0.660$, $R^2 = 0.957$ and $R^2_{pred} = 0.701$ in CoMFA model, and $Q^2 = 0.685$, $R^2 = 0.969$ with $R^2_{pred} = 0.829$ in CoMSIA model. Molecular docking provides further insights into the binding modes of these BTDs with the *CA* XII protein. The results indicated that key residues Thr199, Thr200, Gln92, Asn62 and Leu198 could interact with BTDs by hydrogen bonds or hydrophobic interactions, which might be significant for the activity. The information obtained will be very helpful for designing new derivatives with high anti-hCA XII activity.

Keywords: 3D-QSAR, CoMFA, CoMSIA, molecular docking, drug design, carbonic anhydrase.

INTRODUCTION

CARBONIC anhydrases (CAs) play a crucial role in catalyzing the hydration of CO_2 to bicarbonate and protons, alongside other hydrolytic reactions.[1] The hydration of carbon dioxide is essential in several physiological processes, including respiration, pH regulation, CO_2 balance, fat synthesis, sugar production, and tumor formation.[2] As of the current date, researchers have identified a total of seven distinct genetic families of carbonic anhydrases (*α, β, γ, δ, ζ, η* and *ϑ*). The human carbonic anhydrases (hCAs) are classified under the *α*-class of carbonic anhydrases, which comprises fifteen isoforms (hCA *I* – hCA *XV*).[3]

The active site of carbonic anhydrase (CA) is located in a deep cavity of 15 Å, at the bottom of this cavity a crucial Zn^{2+} ion is coordinated by three histidine residues (His94, His96, His119) and one water molecule or hydroxide anion. The catalytic site consists of distinct hydrophilic and hydrophobic regions.[4] The three conserved histidine residues and zinc, along with Thr 199, facilitate the binding of CA inhibitors specially sulfonamides and related structures (sulfamates, sulfamides). The inhibitors coordinate with zinc through a negatively charged nitrogen atom, while the remaining hydrogen forms a hydrogen bond with the hydroxy group of Thr 199.[5]

Human carbonic anhydrases (hCAs) XII is commonly found in various healthy tissues like the endometrium, colon, kidney, and eye.[6] Its significant involvement in advancing tumor growth, invasiveness, metastasis, and resistance to standard cancer treatments often leads to poor patient outcomes. Inhibitors targeting CA XII have demonstrated effectiveness in curtailing primary tumor development, invasion, metastasis, and reducing the amount of cancer stem cells.[7] Several of these inhibitors

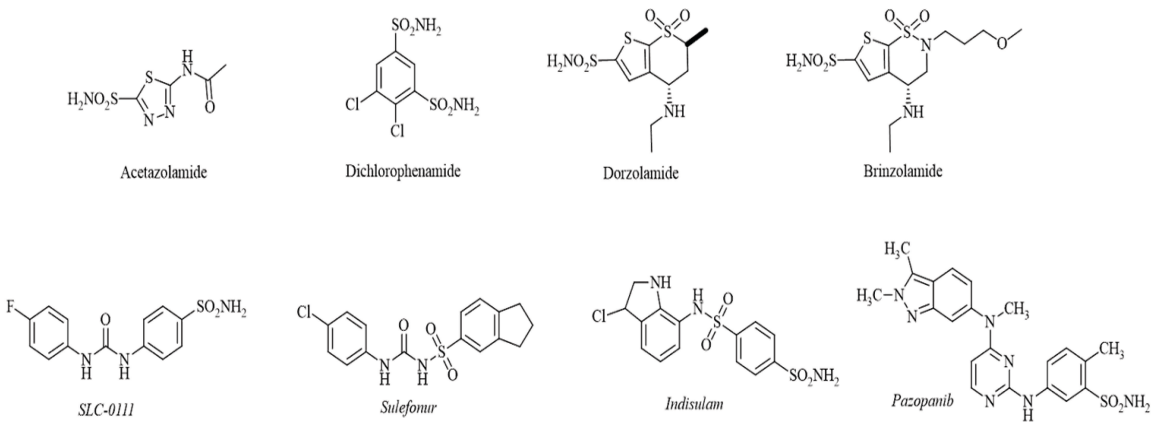

Figure 1. Structure of clinically used carbonic anhydrase inhibitor drugs.

have been evaluated as potential anticancer drug candidates, including SLC-0111, Sulofenur, Indisulam, and Pozapanib (Figure 1), and are currently undergoing anticancer clinical trials.[8]

Computer-aided drug design (CADD) has significantly enhanced the efficacy of drug design and offered innovative solutions for treating persistent ailments.[9] It has been developed and widely used for anticancer, anti-HCV, anti-inflammatory, and anti-AIDS drugs.[10]

The three-dimensional quantitative structure-activity relationship (3D-QSAR) methodology is widely considered one of the most efficient CADD approaches for understanding the mechanisms of drug action and developing new drugs, it involves a quantitative correlation between the molecular structures or properties and the changes in biological activity.[11] Furthermore, molecular docking serves as a powerful tool to compute protein ligand interactions and generate 3D graphical representations, aiding in a more profound understanding of the molecular binding mechanism.[12] Currently, 3D-QSAR approaches, such as comparative molecular field analysis (CoMFA) and comparative molecular similarity indices analysis (CoMSIA) studies are extensively utilized to understand the pharmacological properties of compounds under investigation and for developing new drugs. 3D-QSAR analyses elucidate both favorable and unfavorable zones affecting biological activity.[13] Moreover, molecular docking provides diverse orientations of ligands inside the active region, which helps researchers to develop potential hypotheses about the probable receptor-ligand interactions.[14]

In recent years, several studies have focused on the prediction of novel carbonic anhydrase inhibitors, to identify effective compounds that can modulate the activity of this vital enzyme. Researchers use advanced techniques and Computer-Aided Drug Design (CAAD) methodologies such as virtual screening, *multi*D-QSAR, Hologram QSAR (HQSAR), Topomer-CoMFA, DFT, molecular docking, ADMET and molecular dynamic simulations to enhance the accuracy of their predictions and to discover new therapeutic options.[15] In this context, many important results have been achieved using 3D-QSAR methods such as CoMFA and CoMSIA, along with molecular docking and ADMET analyses, by many researchers including Nilewar,[16] Abdizadeh,[17] Singh,[18] and others.[19,20]

Nilewar's group reported molecular modeling studies on aromatic acid esters for carbonic anhydrase inhibitory activity using several computational techniques (CoMFA, CoMSIA, Topomer CoMFA, and HQSAR). The team conducted a thorough 2D (HQSAR) and 3D (CoMFA and CoMSIA) analysis of the dataset, and based on the results, they established a structure-activity relationship.[16] In 2024, Saravanan and his team developed pharmacophore modeling-based in silico analysis to find selective chemotypes acting as hCA inhibitors that could be used in cancer treatment. The results obtained demonstrate outstanding potential for hCA IX inhibitory action.[16]

In this study, we utilized twenty BTD compounds to develop an accurate 3D-QSAR model. Our aim was to understand the inhibitory activity of these compounds by examining their structural features. The creation of contour maps allowed us to visualize the relationships between these features and the inhibit ory activity. Overall, our findings revealed the intricate connections between structural features and inhibitory activity. The interactions between the newly designed compounds with higher predicted activities and receptor protein was investigated using molecular docking. Finally, the inhibitors were selected by ADMET and bioavailability prediction. This study serves as a crucial reference and guide for the future emergence and advancement of innovative, wide-ranging, and highly potent carbonic anhydrase inhibitors.

EXPERIMENTAL

Data Sets and Biological Activities

The optimal minimum number of compounds required for the effective construction of a 3D-QSAR model, utilizing methods such as CoMFA and CoMSIA, is approximately 15 molecules.[21,22] Based on this guideline, a significant number of researchers have successfully employed datasets with less than twenty compounds to create models with respectable predictive power.[23–25] In this study, we have carefully chosen 20 benzothiadiazin-3-one 1,1-dioxides derivatives (BTDs) as novel inhibitors of Carbonic Anhydrase XII (CA XII) with known inhibition constants (K_i) values ranging from 15.5 to 764 nM. These molecules were selected from published literature reports for the present molecular simulation.[26] The inhibitory activity (K_i) was initially converted to negative logarithmic units (pK_i) for analysis. Moreover, 3D-QSAR models were developed using the proposed molecules; 16 compounds were chosen randomly to create a quantitative model (training set), while the remaining four compounds were used to assess the model's accuracy (test set). The structures of the 20 compounds along with their biological activity can be found in Table 1.

Table 1. Chemical structures and anti-CA XII activities of BTDs derivatives.

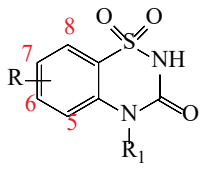

Code	R	R_1	K_i / nM	pK_i
1*	H	H	53.1	7.27
2	5-CH_3	H	69.3	7.16
3	7-CH_3	H	74.3	7.13
4*	5,7-diCH_3	H	38.3	7.42
5	5,8-diCH_3	H	458.7	6.34
6	6,8-diCH_3	H	764	6.12
7	5-F	H	42.7	7.37
8*	7-F	H	24.9	7.60
9	5-Cl	H	42.5	7.37
10	7-Cl	H	70.8	7.15
11	5-Br	H	75.8	7.12
12	7-Br	H	96.6	7.02
13	7-OCH_3	H	64.5	7.19
14	5,6-Benzo	H	104.9	6.98
15	H	CH_3	181.5	6.74
16	7-Cl	CH_3	325.7	6.49
17	5-CH_2-CH_3	H	247.2	6.61
18	5-COOH	H	27	7.57
19*	7-COOH	H	15.5	7.81
20	7-OH	H	34.6	7.46

* test set

Molecular Modelling and Alignment

All proposed compounds were modeled using SYBYLX 2.0 software package (Tripos Inc, Saint Louis, MO, USA. https://www.tripos.com/), on windows 10.0, 64 bits workstation. The sketched benzothiadiazin-3-one 1,1-dioxides derivatives (BTDs) module was minimized using the Tripos force field and by applying Gasteiger-Hückel charges. The maximum number of iterations was 1000, and the gradient energy convergence value was set to 0.005 kcal mol^{-1} Å.[27]

In Figure 2, twenty compounds of benzothiadiazin-3-one 1,1-dioxides derivatives were aligned by the distilling alignment technique available in SYBYL to the common core utilizing molecule 19 (the most active molecule in the data set) as a template.[28]

Construction of CoMFA and CoMSIA Models

The local physical and chemical properties influencing the ligand-receptor interaction have been examined through 3D-QSAR techniques. CoMFA fields were computed utilizing sp3 carbon probe with +1 charge to evaluate steric field energies and electrostatic fields. In addition, it figures out similarity indices for each compound in the dataset that has been aligned using specific methods. CoMSIA employs a Gaussian-like distance dependence function between the probe and the molecule´s atoms to prevent singularities at atomic positions and excessive potential energy fluctuations for grids.[29]

Partial Least Squares (PLS) Analysis

The PLS analyses are implemented using two techniques: cross-validation leave-one-out and non-cross-validation. In the first stage, PLS analysis uses a cross-validation leave-one-out technique to determine the cross-validation correlation coefficient (Q^2) and the optimal number of components (ONC).

In the second step, the PLS analysis uses the non-cross-validation technique to determine the coefficient of determination (R^2), standard error of estimation (SEE) and Fischer statistical test value (F). A model is eligible to be selected for further analysis if the following requirements are satisfied: $Q^2 > 0.5$, ONC < 10, $R^2 > 0.6$, SEE << 1 and F >> 10.[25]

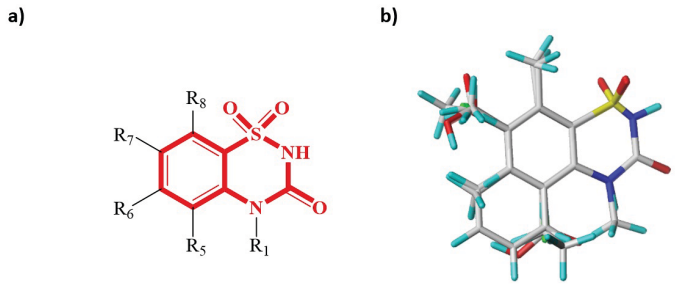

Figure 2. Alignment of dataset: (a) The common substructure (red) used in database alignment; (b) The alignment result based on the common substructure of compound **19**. Molecules are colored in white for common C, blue for N, red for O, yellow for S, cyan for H, green for F and Cl.

Validation of CoMFA and CoMSIA Models

The primary objective of employing a 3D-QSAR model is to estimate the activity of non-synthetic compounds based on their predictive power and robustness. For this reason, the recommended models have been submitted to additional validation. Four compounds have been employed in the external validation approach as test set molecules. Similarly to the training set, these molecules were sketched and optimized by the same method. The pK_i of the four studied molecules used in the validation process was calculated using the recommended models. The prediction capacity of the elaborated models was investigated by determining the predictive correlation coefficient R^2_{pred} of test set as external validation parameter. As a rule, $R^2_{pred} > 0.6$ show the 3D-QSAR models have an excellent external predictive ability.[30]

Molecular Docking

Molecular docking is a widely used computational approach in studying the potential interaction between candidate drugs and the active site of a protein or enzyme.[31] The crystal structure of human carbonic anhydrase XII (hCA XII) protein in complex with acetazolamide (PDB ID: 1JD0) was downloaded from RCSB Protein Data Bank (https://www.rcsb.org/). The process of molecular docking ligand-receptor involves three main steps: preparation of the protein and ligand, creation of the receptor grid, and the molecular docking process.[32] We used AutoDock Vina 1.1.2 software for conducting molecular docking investigations.[33] The grid was positioned with center coordinates x (−14.293), y (−6.726), and z (20.795), with grid spacing set at 25 Å using standard docking parameters.[34]

Furthermore, BIOVIA Discovery Studio Visualizer was employed for the visualization and assessment of the 2D and 3D interactions within the protein-ligand complexes (https://www.3ds.com/products/biovia/discovery-studio/visualization).

ADMET and Drug-likeness Prediction

The physicochemical and biological properties of a small molecule play a main role in determining the potential efficacy of a candidate drug.[35] By incorporating Lipinski's rules and utilizing the ADMETlab 3.0 web server (http://admetlab3.scbdd.com/), we can effectively evaluate the usability of the molecule.[36] The admetSAR web server (https://lmmd.ecust.edu.cn/admetsar2) was utilized to determine the pharmacokinetic (oral bioavailability) and ADMET (absorption, distribution, metabolism, excretion, and toxicity) parameters of selected drugs.[37] Criteria for assessing oral absorption characteristics include molecular weight (M_w) ≤ 500, logP of 5, hydrogen bond donors (DBL) of 5, number of hydrogen bond acceptors (HBA) ≤ 10, and topological polar surface area (TPS) 140. Meeting these criteria indicates oral bioavailability.[38]

RESULTS AND DISCUSSION

Analysis of CoMFA and CoMSIA Model

CoMFA and CoMSIA models are built using different subsets of training and test compounds. The computational outcomes derived from the application of Partial Least Squares (PLS) analysis on these models are summarized in Table 2. The stability of the CoMFA and CoMSIA models can be evaluated by Q^2, R^2, ONC, F, SEE and R^2_{pred} values. It is generally considered that models with $Q^2 > 0.5$ and $R^2 > 0.6$ have good internal validation ability, and those with $R^2_{pred} > 0.6$ have good external prediction ability. The best models were also evaluated using low optimal number of component ONC and low standard error estimate values.[39]

In the present study, the generated CoMFA-S model shows the best parameters compared to CoMFA-SE and CoMFA-E models with the highest internal validation coefficients ($Q^2 = 0.660$ and $R^2 = 0.957$) and good external prediction coefficient ($R^2_{pred} = 0.701$). In addition, the

Table 2. The statistic results of CoMFA and CoMSIA models.

Descriptors			Parameters					
			Q^2	R^2	SEE	ONC	F	R^2_{pred}
CoMFA	**S**		**0.660**	**0.957**	**0.101**	**4**	**42.249**	**0.701**
CoMFA	E		0.216	0.641	0.269	2	8.447	0.319
CoMFA	S	E	0.536	0.961	0.097	4	22.161	0.552
CoMSIA	S		0.594	0.891	0.161	4	38.169	0.680
CoMSIA	E		0.301	0.652	0.265	2	10.460	0.368
CoMSIA	**H**		**0.685**	**0.969**	**0.087**	**4**	**87.298**	**0.829**
CoMSIA	D		0.012	0.467	0.341	3	12.668	0.413
CoMSIA	A		0.029	0.255	0.388	2	6.817	0.275
CoMSIA	S	E	0.352	0.755	0.222	2	17.243	0.489
CoMSIA	S	H	0.669	0.979	0.071	4	80.198	0.817
CoMSIA	S	D	0.385	0.914	0.143	4	56.704	0.759
CoMSIA	S	A	0.483	0.935	0.125	4	93.117	0.838
CoMSIA	E	H	0.522	0.949	0.113	4	51.982	0.743
CoMSIA	E	D	0.297	0.514	0.302	1	11.952	0.399
CoMSIA	E	A	0.315	0.657	0.263	2	15.020	0.455
CoMSIA	H	D	0.533	0.952	0.107	4	86.227	0.827
CoMSIA	H	A	0.615	0.954	0.104	4	96.746	0.843
CoMSIA	D	A	0.009	0.282	0.367	1	6.965	0.279

S = Steric field, E = Electrostatic field, H = Hydrophobic field, D = Hydrogen bond donor field, A = Acceptor field, Q^2 = Leave one out (LOO) cross-validated correlation coefficient, R^2 = Non-cross validated correlation coefficient, SEE = Standard error of estimation, ONC = number of optimum components, F = Fischer-test value, R^2_{pred} = Predictive correlation coefficient of test set (external validation parameter). Note: Bold line indicates best significant optimized model.

CoMFA-S model describing carbonic anhydrase inhibitors possesses a low standard error estimate (SEE) value of 0.101 with an optimum number of components (ONC) of four. All validation parameters of the CoMFA-S model are eligible and indicating that the model has good statistical significance.

In order to find the optimum CoMSIA, different models were constructed by the combination of the steric field (S), electrostatic field (E), hydrophobic field (H), hydrogen bond donor field (D) and acceptor field (A) and the statistical values are listed in Table 2.

Among the possible field combinations, the CoMSIA-H model stood out with the highest Q^2 value (Q^2 = 0.685) with R^2 = 0.969 and an outstanding external prediction parameter (R^2_{pred} = 0.829). Furthermore, the CoMSIA-H model demonstrates strong predictive ability and credibility with validation data indicating SEE = 0.087, and ONC = 4. CoMSIA-H was identified as the most optimal CoMSIA model and selected for further analysis. The calculated pK_i values of compounds with the obtained CoMFA-S and CoMSIA-H models are listed in Table 3.

The relationships between the experimental pK_i values *vs.* calculated pK_i values are plotted in Figure 3. Most compounds in the CoMFA-S and CoMSIA-H models align at or near the trend line, this alignment demonstrates a strong fit between the compound's actual and predicted activities, as reflected by pK_i values.

CoMFA and CoMSIA Contour Maps

The contour map of the CoMFA model is shown in Figure 4, with compound 19 as reference. In the CoMFA steric field, the green surfaces indicate that adding bulky groups would enhance biological activity, while the yellow surfaces suggest that adding bulky groups might not be favorable. A wide green surface is located near the 5 and 6 groups, indicating that the presence of a bulky group in those positions could potentially enhance the activity. This is confirmed by the following activity order: Compound 2 with methyl group at 5 (pK_i = 7.16) > compound 3 with methyl group at 7 (pK_i = 7.13) and compound 14 (with a benzene ring at 5 and 6) (pK_i = 6.98) > compound 6 (with dimethyl at 6 and 8) (pK_i = 6.12).

Table 3. Experimental and predicted pK_i with errors of the training and test sets using CoMFA and CoMSIA models.

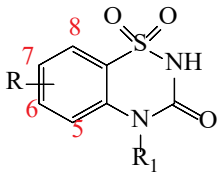

Code	R	R_1	p$K_{i_{exp}}$	Predicted Activity (pK_i)			
				CoMFA-S		CoMSIA-H	
				p$K_{i_{pred}}$	Error	p$K_{i_{pred}}$	Error
1	H	H	7.27	7.37	0.10	7.29	0.02
2	5-CH3	H	7.16	7.02	–0.14	7.02	–0.14
3	7-CH3	H	7.13	7.08	–0.05	7.18	0.05
4	5,7-diCH3	H	7.42	6.72	–0.69	6.79	–0.63
5	5,8-diCH3	H	6.34	6.35	0.01	6.32	–0.02
6	6,8-diCH3	H	6.12	6.11	–0.01	6.14	0.02
7	5-F	H	7.37	7.40	0.03	7.29	–0.08
8	7-F	H	7.60	7.35	–0.25	7.25	–0.35
9	5-Cl	H	7.37	7.38	0.01	7.27	–0.10
10	7-Cl	H	7.15	7.19	0.04	7.13	–0.02
11	5-Br	H	7.12	7.28	0.16	7.25	0.13
12	7-Br	H	7.02	7.16	0.15	7.04	0.03
13	7-OCH3	H	7.19	7.13	–0.06	7.29	0.10
14	5,6-Benzo	H	6.98	7.01	0.03	6.98	0.00
15	H	CH3	6.74	6.73	–0.01	6.68	–0.06
16	7-Cl	CH3	6.49	6.54	0.06	6.51	0.02
17	5-CH2-CH3	H	6.61	6.59	–0.01	6.69	0.08
18	5-COOH	H	7.57	7.55	–0.02	7.61	0.04
19	7-COOH	H	7.81	7.05	–0.76	7.45	–0.36
20	7-OH	H	7.46	7.28	–0.18	7.41	–0.05

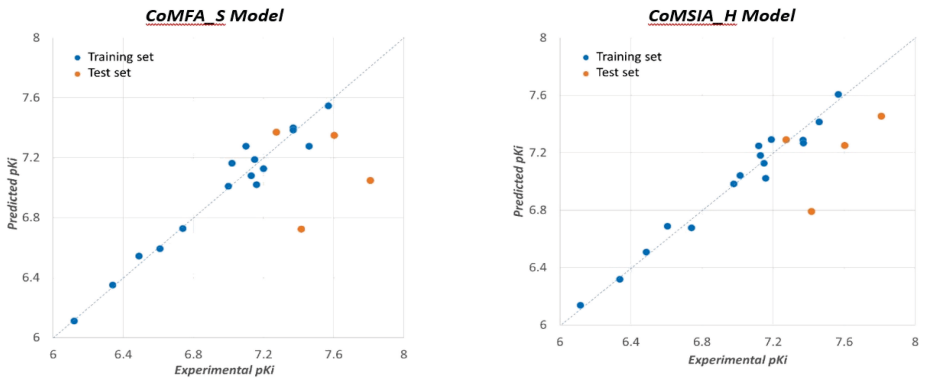

Figure 3. The plot of the correlation between the experimental and predicted activity based on QSAR model of training and test set.

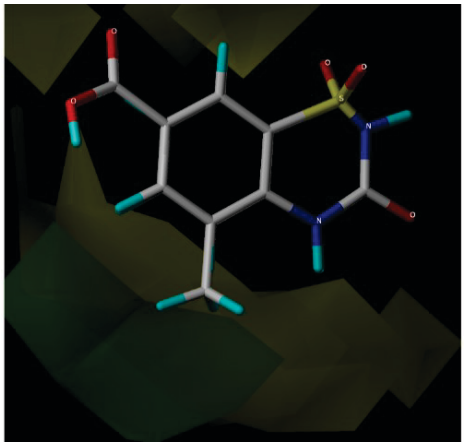

Figure 4. Steric contours of CoMFA based on compound 19.

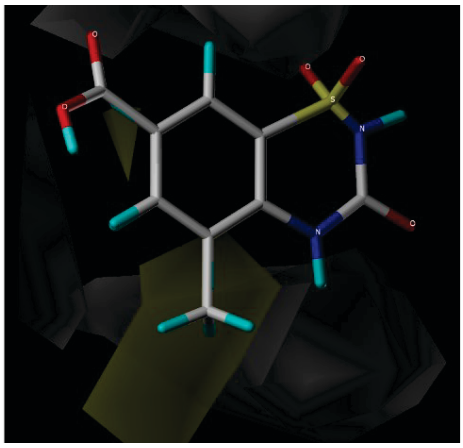

Figure 5. Hydrophobic contour of CoMSIA based on compound 19.

Figure 5 displays the contour maps of the CoMSIA model. In general, a hydrophobic substitution would be favorable for the activity on the yellow surface and unfavorable for the white surface. Clearly, placing a hydrophobic group near the 5 group enhances inhibitory activity, as indicated by the following activity order: Compound 7 with Fluorine group at 5 (pK_i = 7.37) > compound 3 with methyl group at 5 (pK_i = 7.13) and compound 10 with a Chloro at 7 (pK_i = 7.15) > compound 3 with methyl at 7 (pK_i = 7.13).

Design of New BTD Derivatives

The summary of the structure-activity relationship (SAR) Figure 6 provides a comprehensive abstraction of all the information obtained from the CoMFA and CoMSIA contour maps results. This information is extremely valuable as it helps in identifying the specific regions that are responsible for either enhancing or reducing the activity. This will guide us in creating new BTDs compounds with stronger effects. As noted in Figure 6, the addition of bulky groups at the sixth position, hydrophobic groups at the seventh position and bulky hydrophobic groups at the fifth position will enhance the activity of the proposed compounds.

The chemical structure of four new inhibitors and their predicted activity values are illustrated in Table 4. In general, most proposed inhibitors show potent predicted activity, and are therefore considered to be good inhibitors.

Molecular Docking Study

In the current research, we conducted molecular docking analysis to examine the binding pattern of the designed inhibitors BTD (**1**–**4**) with CA XII (PDB: 1JD0), a key mediator of several signaling pathways that are involved in cancer

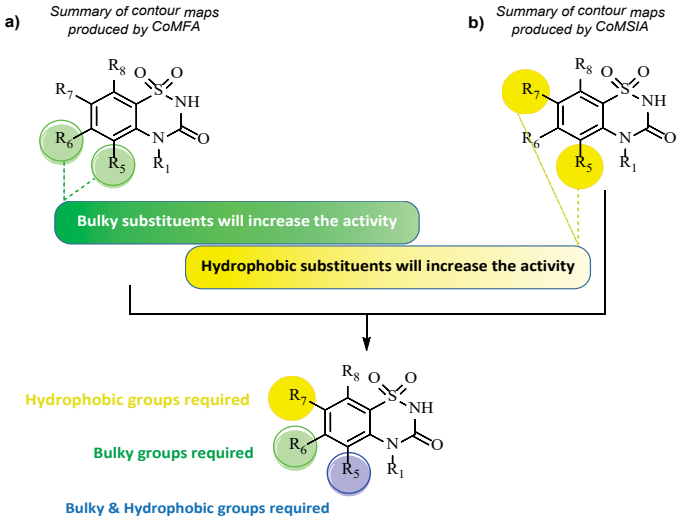

Figure 6. Suggested structural modifications of BTD derivatives for designing of more potent and selective CA XII inhibitors.

Table 4. Structures of new molecules and their pK_i obtained by CoMFA and CoMSIA model.

		Predicted activity (pK_i)	
Code	R	CoMFA-S	CoMSIA-H
BTD-**1**	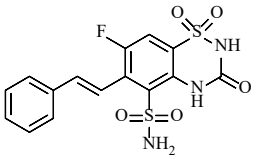	7.85	7.24
BTD-**2**	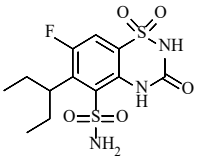	7.97	7.64
BTD-**3**	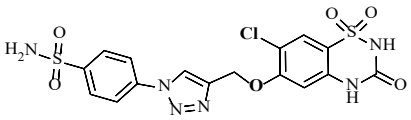	8.22	7.79
BTD-**4**	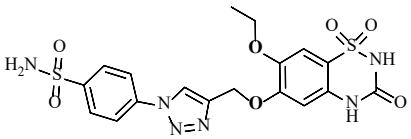	7.96	7.56

Figure 7. Crystal structure of human carbonic anhydrase XII complexed with AAZ (PDB: 1JD0).

development. Our aim was to compare these inhibitors with the well-known drug for carbonic anhydrase treatment acetazolamide (AAZ), and the most potent compound in the studied molecules compound **19**.

The binding affinities and interactions resulting from docking the CA XII receptor with the reference ligand AAZ, compound 19, and four (BTD) derivatives are provided in Table 5.

Our findings reveal that the complexes formed between the CA XII receptor and our specially designed compounds exhibit good stability compared to those formed with the reference ligand AAZ (binding energy of –9.14 kcal mol^{-1}), and compound 19 (–7.60 kcal mol^{-1}). Consequently, these novel molecules show promise inhibitory efficacy against the CA XII enzyme ranging from –8.40 to –9.10 kcal mol^{-1}.

Table 5. Docking findings of the reference molecule AAZ, compound **19** and the newly designed drug-candidates.

Compounds	Estimated Free Binding Energy / kcal mol^{-1}	Residues Involved in H-Bond Interactions	Residues Involved in Hydrophobic Interactions
AAZ (Acetazolamide) (Ref. ligand)	–9.14	Thr199, Thr200, Gln92, Asn62	Val121, Val143, Leu198, Trp209
compound **19**	–7.60	Thr199, Thr200, Gln92	Val121, Leu198, His94
BTD-**1**	–8.50	Thr199, Thr200, Gln92,Asn62	Ala131, Val121, Glu106, Leu198, His96
BTD-**2**	–8.40	Thr199, Thr200, Gln92,Asn62	Leu198, His96, His94
BTD-**3**	–9.00	Thr199, Thr200, Gln92,Asn62	Trp5, Val121, Pro202, Leu198, His96
BTD-**4**	–8.40	Thr199, Thr91, Gln92	Leu198, His94,Lys67

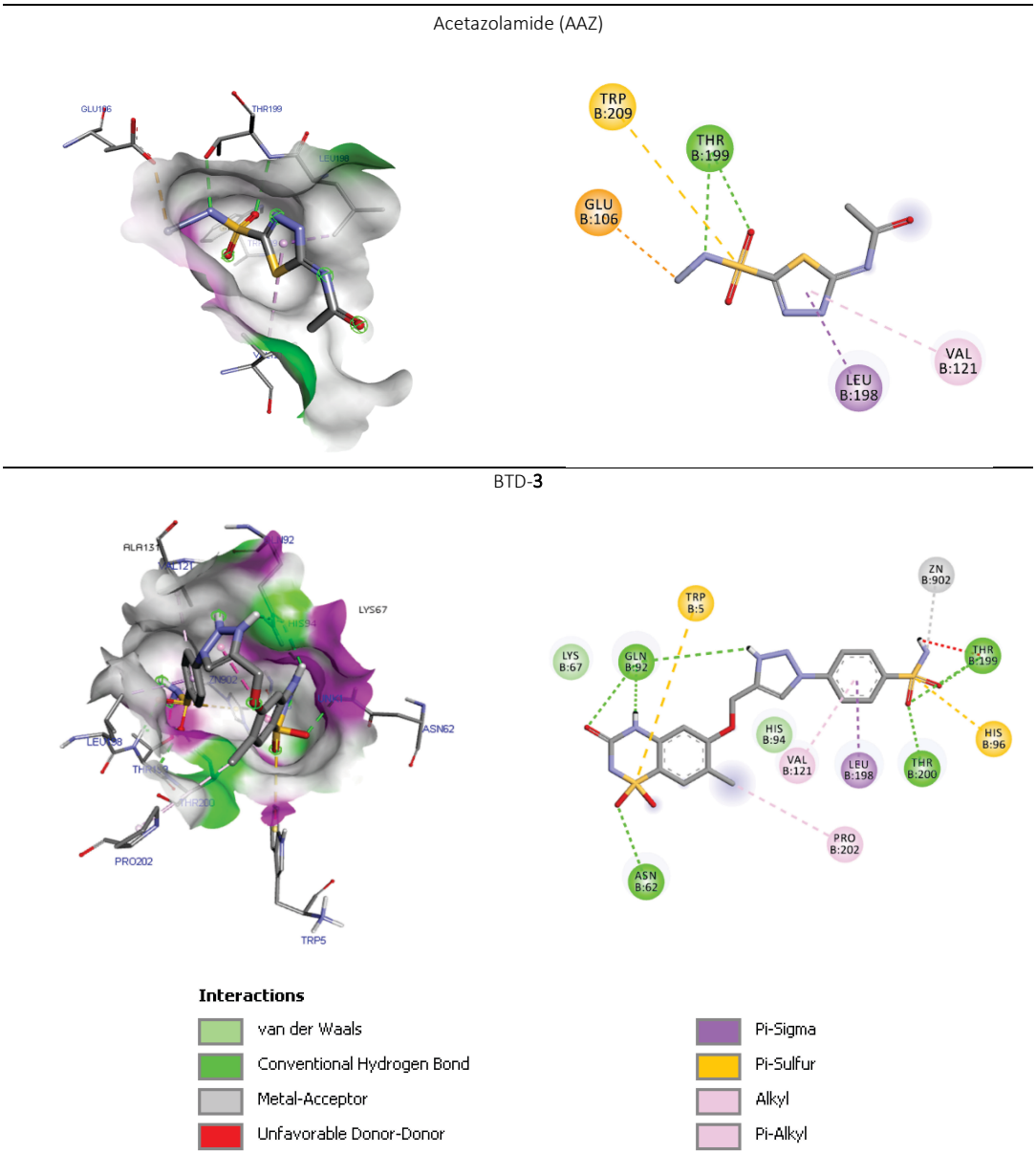

Figure 8. Molecular docking results: (a) 3D view of binding site interactions; (b) 2D view of the binding conformation.

The 2-D and 3-D binding interactions of the reference ligand AAZ, compounds BTD-(**1**–**4**) and compound 19 with the CA XII receptor (PDB: 1JD0) are illustrated in Figure 8 and 9. When compared to AAZ and compound 19, compounds BTD-(**1**–**4**) demonstrated similar H-bond interaction profiles with amino acid residues Thr199 and Gln92 as well as hydrophobic interactions with Leu198.

The most active designed compound BTD-**3** (pK_i = 8.22) stabilized in the cavity of the receptor (PDB code: 1JD0) by six hydrogen bond interactions with Thr199, Thr200, Gln92 and Asn62 similar to AAZ as a standard drug of CA XII.

The three compounds BTD-**1**, BTD-**2**, and BTD-**4** interact with the CA XII receptor through a network of hydrogen bonds with (Thr199, Thr200, Gln92 and Asn62), (Thr199, Thr200, Gln92 and Asn62) and (Thr199, Thr91 and Gln92), respectively. Moreover, compounds BTD-**1** to BTD-**4** exhibit hydrophobic interactions with residue Leu198 similar to the co-crystalized ligand (AAZ).

This means that the presence of these amino acids is essential for inhibiting CA XII. Based on the results obtained from molecular docking, compounds BTD (**1**–**4**) show potential as effective inhibitors of carbonic anhydrase XII when compared to standard drugs like AAZ.

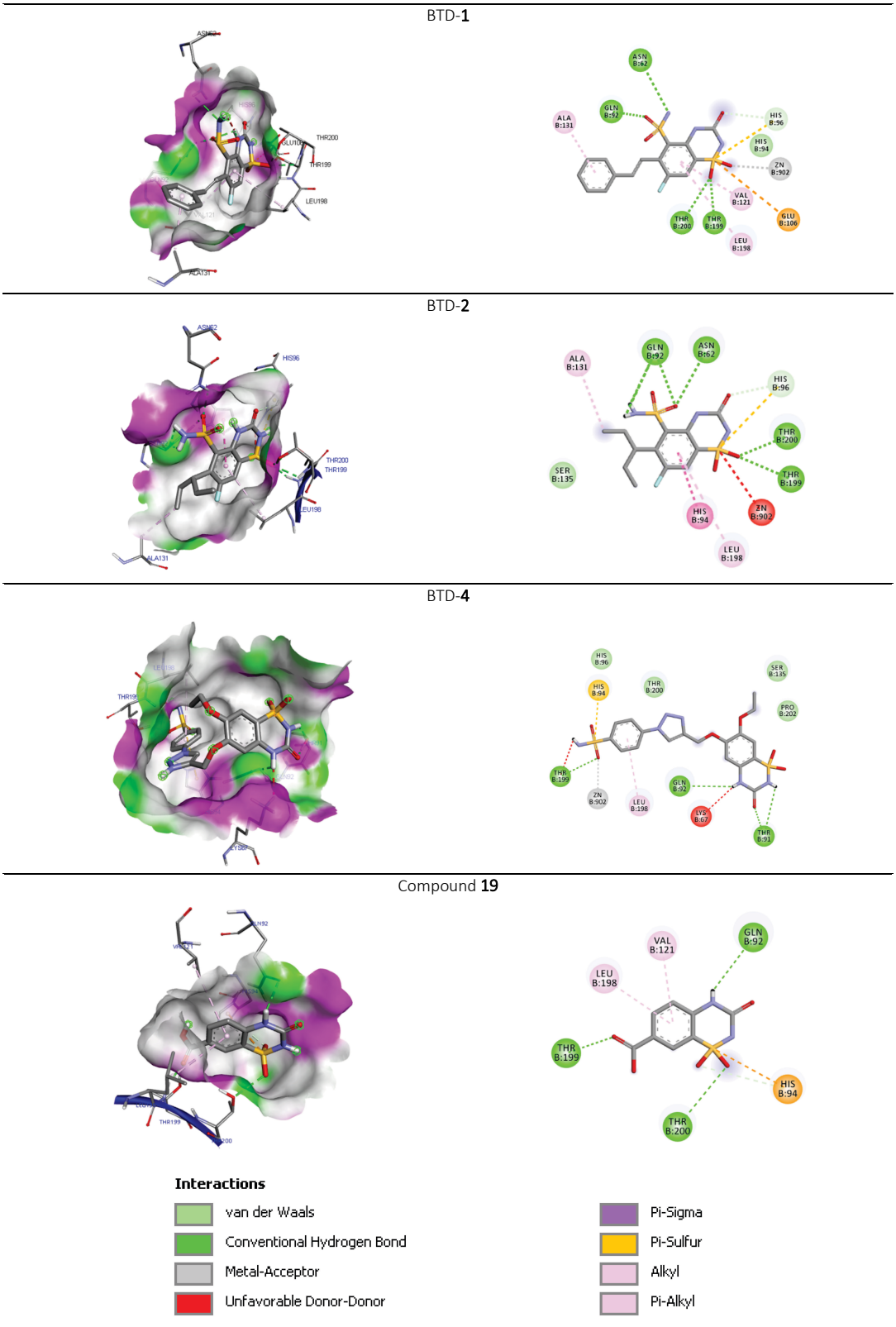

Figure 9. Molecular docking results: 3D view of binding site interactions and 2D view of the binding conformation.

ADMET Analysis

ADMET (Absorption, Distribution, Metabolism, Excretion, and Toxicity) is currently at the forefront of innovative pharmaceutical research and development.[40] The ADMET analysis is very important during the early stages of drug development as it aims to improve the pharmacokinetic properties of ineffective compounds.[41] In our study, all the compounds show positive results for blood brain barrier (BBB) criteria and human intestinal absorption values. As shown in Table 6, all of the drugs pass the human intestinal CACO–2 cell monolayer assay (*in vitro* model).

According to the literature, inhibiting p-glycoprotein can interfere with the drug permeability, absorption, metabolism, and retention.[42] P-glycoprotein serves as an efflux transporter that plays a main role in pumping the drug back into the gut lumen.[43] When P-glycoprotein is induced, it will decrease the bioavailability of the drug, and vice versa. All the analogues in this study were found to be p-glycoprotein non-inhibitors. Furthermore, all compounds showed non-carcinogenic properties, falling within Class III acute oral toxicity.[44]

It is important to note that the inhibition of the human Ether-a-go-go Related Gene (hERG) potassium channel by these analogues could potentially lead to a prolonged QT interval. [45] Fortunately, all of the derivatives showed only weak inhibitory effects on hERG. Moreover, all the compounds are metabolized by CYP4502C9 isoenzymes. The CYP4502C9 *iso*enzymes are important for about 90 % of oxidative metabolic reactions. Thus, most of the derivatives have shown a good oral bioavailability.[46]

Lipinski's Rule Prediction

The drug-likeness criteria of Lipinski's rule of five (M_w < 500, logP < 5, H-bond donors ≤ 5 and H-bond acceptors ≤ 10, and rotatable bonds ≤ 10) were shown in Table 7.REF Lipinski's rule of five is strictly followed by the four compounds, demonstrating their robust drug-like characteristics.[38]

In assessing the drug-likeness of the novel BTD derivatives, the physicochemical parameters of the molecules are usually related to some filter variants. Therefore, relevant physicochemical parameters generated from the ADMETlab 2.0 web server were assessed using numerous drug-likeness rules such as Lipinski's rule, Pfizer's rule, GSK's rule, and Golden triangle rule as presented in Figure 10.

The physicochemical properties for the four compounds BTD (**1**–**4**) are within the upper limit (brown) and lower limit (red) as presented in the radar charts accordingly.

Table 6. ADMET prediction of newly designed compounds.

	Absorption		Distribution			Metabolism	Toxicity		
Name	HIA	C2P	BBB	P-GpI	P-GpS	CYP450 2C9	hERG	Carcinogen	AOT
AAZ	+(0.92)	+(0.78)	+(0.94)	NI (0.93)	0.84	I (0.91)	WI (0.99)	NC (0.80)	III
19	+(0.66)	+(0.63)	+(0.69)	NI (0.99)	0.68	I (0.57)	WI (0.99)	NC (0.78)	III
BTD-**1**	+(0.88)	+(0.69)	+(0.85)	NI (0.97)	0.64	I (0.61)	WI (0.99)	NC (0.80)	III
BTD-**2**	+(0.89)	+(0.66)	+(0.80)	NI (0.97)	0.53	I (0.62)	WI (0.99)	NC (0.74)	III
BTD-**3**	+(0.98)	+(0.59)	+(0.81)	NI (0.68)	0.63	I (0.52)	WI (0.94)	NC (0.65)	III
BTD-**4**	+(0.99)	+(0.58)	+(0.74)	NI (0.88)	0.55	I (0.51)	WI (0.97)	NC (0.67)	III

HIA = Human intestinal absorption, C2P = CACO-2 permeability, BBB = Blood brain barrier, P-GpI = P-glycoprotein inhibitor, PGpS = P-glycoprotein substrate, CYP450 2C9 = Cytochrome P450 2C9, hERG = human Ether-a-go-go Related Gene, AOT = Acute oral toxicity, I = inhibitor, NI = non-inhibitor, WI = weak inhibitor, NC = non-carcinogen.

Table 7. Lipinski validation of the newly designed drug-candidates.

Compounds	Molecular weight / g mol^{-1}	log(P / mol L^{-1})	H-bond acceptors	H-bond donors	Rotatable bonds	
Lipinski Rule	< 500	< 5	≤ 10	≤ 5	≤ 10	Validation
BTD-**1**	397.02	1.65	8	4	3	Accepted
BTD-**2**	365.05	1.69	8	4	4	Accepted
BTD-**3**	484.00	0.93	12	4	5	Accepted
BTD-**4**	494.50	0.77	13	4	7	Accepted

* If two properties are out of range, a poor absorption or permeability is possible, one is acceptable.

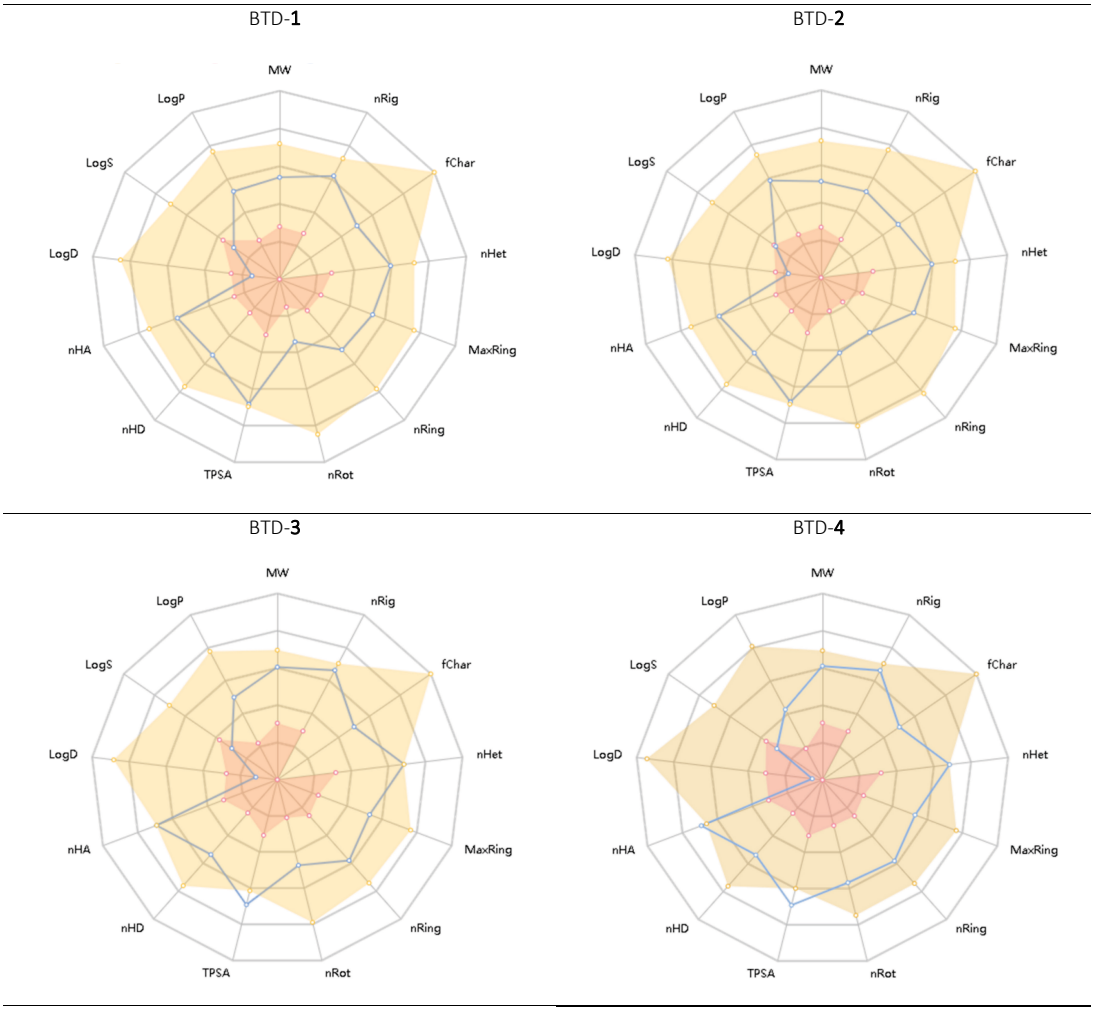

MW = Molecular Weight; nRing = Number of rings; fChar = Formal charge; nHet = Number of heteroatoms; MaxRing = Number of atoms in the biggest ring; nRig = Number of rigid bonds; nRot = Number of rotatable bonds; TPSA = Topological Polar Surface Area; nHD = Number of hydrogen bond donors; nHA = Number of hydrogen bond acceptors; logD = LogP at physiological pH 7.4; logS = Log of the aqueous solubility; logP = Log of the octanol/water partition coefficient.

Figure 10. Physicochemical radar chart of the predicted compounds.

CONCLUSION

In this study, various computational techniques including 3D-QSAR, molecular docking, and ADMET were utilized to investigate BTDs inhibitors. CoMFA and CoMSIA methods were utilized to establish reliable and predictive 3D-QSAR models. The resulting contour maps illustrate the structure-activity relationship of the inhibitors, which are capable of predicting the activity of the external compounds in a reliable manner.

Molecular docking results indicated that key residues Thr199, Thr200, Gln92, Asn62 and Leu198 could interact with BTDs by hydrogen bonds, π–π stackings, or hydrophobic interactions. These interactions might be essential for their affinity with the CA XII protein.

The study utilized 3D-QSAR techniques with molecular docking analysis to create four novel compounds BTD (**1**–**4**) with good anti-carbonic anhydrase properties. These compounds, displaying improved kinetics, promising *in silico* ADMET and drug-likeness evaluations emerge as strong candidates for new CA XII treatments.

Acknowledgment. The authors acknowledge the Scientific and Technical Research Center in Physico-chemical Analysis (CRAPC), Directorate-General for Scientific Research and Technological Development (DGRSDT), and Ministry of Higher Education and Scientific Research in Algeria for their support.

REFERENCES

[1] T. Eysteinsson,H. Gudmundsdottir, A. O. Hardarson, E. Berrino, S. Selleri, C.T. Supuran, F. Carta, *Int. J. Mol. Sci.* **2019**, *20*, 467. https://doi.org/10.3390/ijms20030467

[2] S. Kumar, S. Rulhania, S. Jaswal, V. Monga, *Eur. J. Med. Chem.* **2021**, *209,* 239. https://doi.org/10.3109/14756366.2015.1122001

[3] C. T. Supuran, *J. Enzyme Inhib. Med. Chem.* **2016**, *31*, 345–360. https://doi.org/10.1080/14756366.2016.1241781

[4] Y. Entezari Heravi, H. Sereshti, A. A. Saboury, J. Ghasemi, M. Amirmostofian, C. T. Supuran, *J. Enzyme Inhib. Med. Chem.* **2017**, *32*, 688–700. https://doi.org/10.1080/14756366.2016.1241781

[5] A. Hillebrecht, C. T. Supuran, G. Klebe, *ChemMedChem* **2006**, *1*, 839–853. https://doi.org/10.1002/cmdc.200600083

[6] H. A. Allam, S. H. Fahim, M. F. Abo-Ashour, A. Nocentini, M. E. Elbakry, M. A. Abdelrahman, W. M. Eldehna, H. S. Ibrahim, C. T. Supuran, *Eur. J. Med. Chem.* **2019**, *179*, 547–556. https://doi.org/10.1016/j.ejmech.2019.06.081

[7] S. Giovannuzzi, M. D'ambrosio, C. Luceri, S. M. Osman, M. Pallecchi, G. Bartolucci, A. Nocentini, C. T. Supuran, *Int. J. Mol. Sci.* **2022**, *23*, 461. https://doi.org/10.3390/ijms23010461

[8] H. I. Gul, C. Yamali, H. Sakagami, A. Angeli, J. Leitans, A. Kazaks, K. Tars, D. O. Ozgun, C. T. Supuran, *Bioorg. Chem.* **2018**, *77*, 411–419. https://doi.org/10.1016/j.bioorg.2018.01.021

[9] L. Zhao, H. L. Ciallella, L. M. Aleksunes, H. Zhu, *Drug Discov. Today* **2020**, *25*, 1624–1638. https://doi.org/10.1016/j.drudis.2020.07.005

[10] E. R. Avinash Kumar Paridhi Agarwal, S. G. Kini, *J. Biomol. Struct. Dyn.* **2022**, *40*, 4850–4865. https://doi.org/10.1080/07391102.2020.1862706

[11] A. Tropsha, O. Isayev, A. Varnek, G. Schneider, A. Cherkasov, *Nat. Rev. Drug Discov.* **2024**, *23*, 141–155. https://doi.org/10.1038/s41573-023-00832-0

[12] I. Asiamah,S. A. Obiri, W. Tamekloe, F. A. Armah, L. S. Borquaye, *Sci. Afr.* **2023**, *20*, 01593. https://doi.org/10.1016/j.sciaf.2023.e01593

[13] X. Yu, X. Zhao, Q. Zhang, C. Dai, Q. Huang, L. Zhang, Y. Liu, Y. Shen, Z. Lin, *ChemistrySelect* **2023**, *8*. 3978. https://doi.org/10.1002/slct.202203978

[14] F. Stanzione, I. Giangreco, J. C. Cole, In *Progress in Medicinal Chemistry*, D. R Witty, B. Cox, Eds., Elsevier, **2021**. 60, 273–343. https://doi.org/10.1016/bs.pmch.2021.01.004

[15] H. Haghshenas, B. Kaviani, M. Firouzeh, H. Tavakol, *J. Comput. Chem.* **2021**, *42*, 917–929. https://doi.org/10.1002/jcc.26514

[16] S. S. Nilewar, M. K. Kathiravan, *J. Chemom.* **2014**, *28*, 60–70. https://doi.org/10.1002/cem.2574

[17] R. Abdizadeh, K. Ghatreh-Samani, F. Hadizadeh, T. Abdizadeh, *J. Mol. Struct.* **2021**, *1229*, 129735. https://doi.org/10.1016/j.molstruc.2020.129735

[18] S. Singh, *Curr. Enzym. Inhib.* **2019**, *15*, 69–77. https://doi.org/10.2174/1573408015666190402100338

[19] K. K. Sethi, S. M. Verma, N. Prasanthi, S. K. Sahoo, R. N. Parhi, P. Suresh, *Bioorg. Med. Chem. Lett.* **2010,** *20,* 3089–3093. https://doi.org/10.1016/j.bmcl.2010.03.104

[20] Y. Wang, H. Guo, G. Tang, Q. He, Y. Zhang, Y. Hu, Y. Wang, Z. Lin, *Comput. Biol. Chem.* **2019**, *80*, 234–243. https://doi.org/10.1016/j.compbiolchem.2019.03.005

[21] K. H. Kim, *Mol. Similarity Drug Des.* **1995**, *12,* 291–331. https://doi.org/10.1007/978-94-011-1350-2_12

[22] "QSAR and CoMFA® Manual SYBYL ®-X 2.0," 2012. [Online]. Available: http://www.tripos.com

[23] A. Ghaleb, A. Aouidate, M. Ghamali, A. Sbai, M. Bouachrine, T. Lakhlifi, *J. Mol. Struct.* **2017**, *1145,* 278–284. https://doi.org/10.1016/j.molstruc.2017.05.065

[24] Z Wang , Y Qin, P Wang , Y Yang, Q Wen, X Zhang, H Qiu, Y Duan, Y Wang, Y Sang, H Zhu, *Eur. J. Med. Chem.* **2013,** *66*, 1–11. https://doi.org/10.1016/j.ejmech.2013.04.035

[25] Y. Rena, Z. Wanga, X. Zhanga, H. Qiu, P. Wang, A. Jiangb, H. Zhu, *RSC Adv.* **2015,** *5,* 21445–21454. https://doi.org/10.1039/C4RA10606G

[26] S. Bua, C. Lomelino, A. B. Murray, S. M. Osman, Z. A. Alothman, M. Bozdag, H. A. Abdel-Aziz, W. M. Eldehna, R. McKenna, A. Nocentini, C. T. Supuran, *J. Med. Chem.* **2020**, *63*, 321–333. https://doi.org/10.1021/acs.jmedchem.9b01669

[27] W. P. Purcell, J. A. Singer, *J. Chem. Eng. Data* **1967**, *12*, 235–246. https://doi.org/10.1021/je60033a020

[28] L. El Mchichi, K. Tabti, R. Kasmi, R El-Mernissi, A. El Aissouq, F. En-nahli, A. Belhassan, T. Lakhlifi, M. Bouachrine, *J. Indian Chem. Soc.* **2022**, *99*, 100582. https://doi.org/10.1016/j.jics.2022.100582

[29] A. Zięba, T. Laitinen, J. Z. Patel, A. Poso, A. A. Kaczor, *Int. J. Mol. Sci.* **2021**, *22*, 6108. https://doi.org/10.3390/ijms22116108

[30] N. Zhai, C. Wang, F. Wu, L. Xiong, X. Luo, X. Ju, G. Liu, *Int. J. Mol. Sci.* **2021**, *22*, 8122. https://doi.org/10.3390/ijms22158122

[31] P. C. Agu, C. A. Afiukwa, O. U. Orji, E. M. Ezeh, I. H. Ofoke, C. O. Ogbu, E. I. Ugwuja, P. M. Aja, *Sci. Rep.* **2023**, *13*, 13398. https://doi.org/10.1038/s41598-023-40160-2

[32] K. Onodera, K. Satou, H. Hirota, *J. Chem. Inf. Model.* **2007**, *47*, 1609–1618. https://doi.org/10.1021/ci7000378

[33] N. T. Nguyen, T. H. Nguyen, T. N. H. Pham, N. T. Huy, M. Van Bay, M. Q. Pham, P. C. Nam, V. V. Vu, S. T. Ngo, *J. Chem. Inf. Model* **2020**, *60*, 204–211. https://doi.org/10.1021/acs.jcim.9b00778

[34] V. Y. Tanchuk, V. O. Tanin, A. I. Vovk, G. Poda, G. *Chem. Biol. Drug. Des.* **2016**, *87*, 618–625. https://doi.org/10.1111/cbdd.12697

[35] D. Li, L. Chen, Y. Li, S. Tian, H. Sun, T. Hou, *Mol. Pharm.* **2014**, *11*, 716–726. https://doi.org/10.1021/mp400450m

[36] L. Fu, S. Shi, J. Yi, N. Wang, Y. He, Z. Wu, J. Peng, Y. Deng, W. Wang, C. Wu, A. Lyu, X. Zeng, W. Zhao, T. Hou, D. Cao, *Nucleic Acids Res.* **2024**, *52*, 422–431. https://doi.org/10.1093/nar/gkae236

[37] H. Yang, C. Lou, L. Sun, J. Li, Y. Cai, Z. Wang, W. Li, G. Liu, Y. Tang, *Bioinformatics* **2019**, *35*, 1067–1069. https://doi.org/10.1093/bioinformatics/bty707

[38] Y. Ouyang, J. Huang, Y.-L. Wang, H. Zhong, B.-A. Song, G. Hao, *J. Agric. Food. Chem.* **2021**, *69*, 10761–10773. https://doi.org/10.1021/acs.jafc.1c01460

[39] A. Patel, H. Bhatt, B. Patel, B. *J. Mol. Struct.* **2022**, *1249*, 131636. https://doi.org/10.1016/j.molstruc.2021.131636

[40] E. L. Cáceres, M. Tudor, A. C. Cheng, *Future Med. Chem.* **2020**, *12*, 1995–1999. https://doi.org/10.4155/fmc-2020-0259

[41] S. K. Jha, M. Imran, L. A. Jha, N. Hasan, V. K. Panthi, K. R. Paudel, W. H. Almalki, Y. Mohammed, P. Kesharwani, *Environ. Res.* **2023**, *236*, 116823. https://doi.org/10.1016/j.envres.2023.116823

[42] R. Ohashi, R. Watanabe, T. Esaki, T. Taniguchi, N. Torimoto-Katori, T. Watanabe, Y. Ogasawara, T. Takahashi, M. Tsukimoto, K. Mizuguchi, *Mol. Pharm.* **2019**, *16*, 1851–1863. https://doi.org/10.1021/acs.molpharmaceut.8b01143

[43] K. Gandla, F. Islam, M. Zehravi, A. Karunakaran, I. Sharma, M. A. Haque, S. Kumar, K. Pratyush, S. A. Dhawale, F. Nainu, S. L. Khan, M. R. Islam, K. S. Al-Mugren, F. A. Siddiqui, T. Bin Emran, M. U. Khandaker, *Heliyon* **2023**, *9*, 19454. https://doi.org/10.1016/j.heliyon.2023.e19454

[44] S. Lazzaro, M. A. West, S. Eatemadpour, B. Feng, BM. V. S. Varma, A. D. Rodrigues, C. Temesszentandrási-Ambrus, P. Kovács-Hajdu, Z. Nerada, Z. Gáborik, C. Costales, C. *J. Pharm. Sci.* **2023**, *112*, 1715–1723. https://doi.org/10.1016/j.xphs.2023.01.014

[45] S. Wang, H. Sun, H. Liu, D. Li, Y. Li, T. Hou, *Mol. Pharm.* **2016**, *13*, 2855–2866. https://doi.org/10.1021/acs.molpharmaceut.6b00471

F. Cheng, W. Li, Y. Zhou, J. Shen, Z. Wu, G. Liu, P. W. Lee, Y. Tang, *J. Chem. Inf. Model.* **2012**, *52*, 3099–3105. https://doi.org/10.1021/ci300367a